Acta Mechanica Sinica (2014) 30(5):681–686
DOI 10.1007/s10409-014-0073-2

RESEARCH PAPER

An experimental research on surface oscillation of buoyant-thermocapillary convection in open cylindrical annuli

Li Zhang · Li Duan · Qi Kang

Received: 16 April 2013 / Revised: 10 December 2013 / Accepted: 27 March 2014

Abstract An experiment is carried out on the surface oscillation of buoyant-thermocapillary convection in an open cylindrical annulus. When the radial temperature difference ΔT reaches a critical value ΔT_c, a regular oscillation appears and soon disappears on the open surface, which varies when the liquid layer's thickness h and temperature difference ΔT are varied. With growth of ΔT, dominant frequency of the visible oscillation will grow too but is found within certain frequencies. Driving forces, buoyance and thermocapillarity, are responsible for this phenomanon and the "balance" point is considered to exist when h is between 4.5–5.0 mm. Surface oscillation region is also found restricted within a narrow gap when Bo is smaller than 3.7.

Keywords Cylindrical annulus · Buoyant-thermocapillary convection · Surface oscillation · Critical temperature difference

Nomenclature

h	Layer thickness, mm
d	Depth of cylindrical annuli, mm
R_o	Outer radius of the cylindrical annuli, mm
R_i	Inner radius of the cylindrical annuli, mm
Hr	Heat ratio, $Hr = \frac{R_i}{R_o}$
A	Aspect ratio, $A = \frac{h}{R_o - R_i}$
ΔT	Temperature difference, °C
ΔT_c	Critical temperature difference, °C
ν	Kinematic viscosity, m^2/s
α	Thermal diffusivity, m^2/s
μ	Dynamic viscosity, kg/(m·s)
γ_T	Temperature derivative of surface tension, N/(m·°C)
β	Volume expansion coefficient
ρ	Density, kg/m^3
g	Normal earth gravity, m/s^2
Pr	Prandtl number, $Pr = \frac{\nu}{\alpha}$
Ma	Marangoni number, $Ma = \gamma_T \frac{\Delta T h}{\mu \alpha}$
Ra	Rayleigh number, $Ra = \frac{g\beta h^3 \Delta T}{\alpha \nu}$
Bo	Bond number, $Bo = \frac{\rho g \beta h^2}{\gamma_T}$

The project was supported by the National Natural Science Foundation of China (11032011 and 10972224) and Knowledge Innovation Program of Chinese Academy of Sciences (KJCX2-YW-L08).

L. Zhang · L. Duan · Q. Kang (✉)
National Microgravity Laboratory,
Institute of Mechanics Chinese Academy of Sciences,
100190 Beijing, China
e-mail: kq@imech.ac.cn

1 Introduction

Buoyant-thermocapillary convection has always been a hot topic and of great importance in either crystal growth or science of thin films [1–3]. It has been proved that there exist many flow patterns and transitions during the convection. The experiment performed by Schwabe et al. [4–6] showed that the flow was kept in a stable multi-cell state when the horizontal temperature was small. Then, the flow would become unstable when the temperature difference was increased and the hydrothermal waves would first occur, followed by more complicated oscillatory flows. They also discovered that the LWI had a longer nondimensional wavelength, even one order of magnitude larger than the SWI [7], and two new convective structures in the case of larger dynamic Bond number [8]. Shi et al. [9] did a 3-D numerical simulation of an 1 mm deep model with finite volume method and Li et al. [10–12] did a theoretic calculation on double layers thermocapillary convection using approximate algorithm and got temperature configuration as well as velocity distribution in the main flow region. They also indicated that the buoyancy force destabilizes the thermocapillary convection in the annular pools with depth ranging from

3 to 10 mm with the melt $Pr = 0.011$ [13]. Moreover, Leppinen [14] showed that curvature effects dramatically dictated the order at which convection influences the core region solutions. Duan et al. [15–17] used the interference technique and bar line technique to measure surface deformation of buoyant-thermocapillary convection in a rectangular pool. They found that with increasing temperature gradient, surface deformation for $h = 3.5$ mm and $h = 6.0$ mm were reversed, and the deformation changes were from several microns to 40 μm. Zhu et al. [18] did a related work and revealed that critical ΔT reduced significantly for fluid layer thickness $h < 1.5$ mm, and decreased slowly on the whole for $h > 1.5$ mm.

Recently, Mo et al. [19] performed linear-stability analyses for a two-layer system of thermocapillary flow, and observed two different patterns of interface temperature bifurcation in the region of $0.625 < \varepsilon < 0.75$. It has also been confirmed that both of thermocapillary and thermogravitatory mechanism can be obtained as long as heat related parameters B and ΔT are properly tuned [20]. Bauer et al. [21] concluded from their computations that the structure of the streamlines depended strongly on the magnitude of the ratio of diameter to height.

Surface flow will respond to the mass conservation [3], so the surface pattern is quite closely connected to fluid's inner motion. When the inner convection transits from stable to unstable, surface oscillations will appear. In our work, we have not only discovered the appearance of surface oscillation in an annular pool, but also found its vanish which have not yet been discussed.

2 Experimental apparatus

An annular container is used as the convection cell (Fig. 1): $R_o = 20$ mm, $R_i = 4$ mm, $d = 12$ mm. The liquid used in the gap is 100 cSt silicone oil ($Pr = 909$) with its physical properties given in Table 1. Central rod is a heat source working with thermal resistance inside a copper shell. The outer wall (copper) is cooled by four pieces of semiconductor patch connected to aluminum radiator each. K9 adiabatic glass is fixed at the bottom. So the convection driving force is obtained when a horizontal temperature difference is formed across the gap called capillarity while coupled with vertical buoyancy.

Our measurement system consists of temperature difference establishing section and surface oscillation detector. Temperature gradient between the inner rod and the outer wall is established by the heating and cooling system under control of a DC power supplier. They are both monitored by a two loops meter Eurotherm 3504. A pair of thermocouple are placed along the heating rod and cooling outside edges to ensure a right temperature difference ($0°C \leqslant \Delta T \leqslant 35.0°C$) we are willing to have. As the most important part of surface oscillation detector, a high-precision displacement sensor LK-H008 is set upon the annulus to capture the z-axis displacement of a surface point. The sensor is based on triangulation method (Fig. 2) and can distinguish ±0.01 μm in our experiment. The data acquisition frequency is 5 000 Hz and average sample recording rate is 5 Hz which means we get one average value out of 1 000 per 0.2 second.

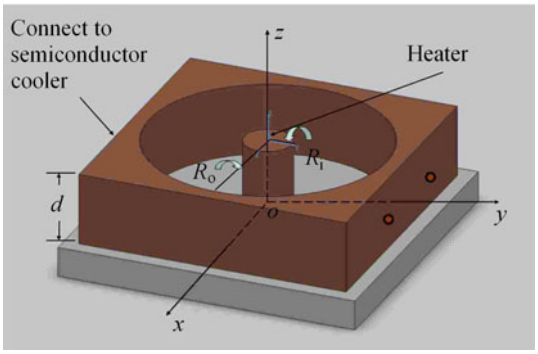

Fig. 1 Sketch of the experimental annulus

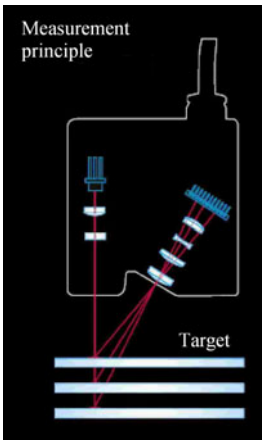

Fig. 2 Sketch of triangulation method for the displacement sensor LK-H008

Table 1 Physical parameters of the test fluid 100 cSt silicone oil

KF96-	ν (25°C)/(mm^2·s^{-1})	ρ (25°C)/(kg·m^{-3})	α (25°C)/(m^2·s^{-1})	σ (25°C)/(mN·m^{-1})	β (25°C–150°C)/K^{-1}	Pr (25°)
100	100	965	1.1×10^{-7}	20.9	9.5×10^{-4}	909.09

3 Oscillation procedures and analysis

During the experiment, we got a series of surface displacement signals at a certain point (6 mm away from the outer edge across the surface) when the thickness of the fluid layer increases from 2.5 to 7.5 mm with an increment of 0.5 mm. According to the typical signal shown in Fig. 3, the whole course can be described as four parts: steady growing-up of displacement, start of oscillation, growing up of the oscillation, disappearance of the oscillation and steady post growing up. The critical starting and disappearing points are identified according to the power spectrum diagram, which can be clearly distinguished.

Let us take $h = 4.5$ mm to detail. When a temperature difference like Fig. 4 is imposed on the fluid layer, we get an original signal (Fig. 5a), an oscillation diagram (Fig. 5b) and a power spectrum diagram (Fig. 5c). We may divide this into four parts based on its behavior to give a clear description, as shown in Fig. 6. Every part contains over 5 000 data points, so it is appropriate for Fast Fourier Transform.

In Part 1, it is 1 100–1 880 s when the temperature difference goes up from 7.1°C to 12.0°C. Nothing can be observed from the time-based signal. But with the FFT diagram we may find four sharps from left to right, they are: $f_1 = 0.018$ Hz, $A_1 = 0.86$ μm, $f_2 = 0.021$ Hz, $A_2 = 1.18$ μm, $f_3 = 0.028$ Hz, $A_3 = 1.46$ μm, $f_4 = 0.048$ Hz, $A_4 = 0.58$ μm.

In Part 2, it is 1 880–3 000 s when the temperature difference stays still at 12°C. We also find four sharps: $f_1 = 0.018$ Hz, $A_1 = 7.30$ μm, $f_2 = 0.021$ Hz, $A_2 = 10.25$ μm, $f_3 = 0.028$ Hz, $A_3 = 4.68$ μm, $f_4 = 0.049$ Hz, $A_4 = 1.63$ μm. They are of no difference but amplitude with the results above. As is believed, the motion of the fluid layer may result from the comprehensive effect of thermocapillarity, buoyancy and the returning flow, so we consider these three factors as the contributors to the frequencies above, though no relative experimental results are obtained to indicate which one is responsible for each frequency correspondingly. Compared with Part 1, f_2 becomes a dominant frequency as its amplitude goes up to 10.25 μm.

In Part 3, it is 3 000–4 400 s when the temperature difference goes up from 12.0°C to 23.7°C. $f_2 = 0.021$ Hz, $A_2 = 6.20$μm, $f_3 = 0.028$ Hz, $A_3 = 8.22$ μm, $f_4 = 0.050$ Hz, $A_4 = 2.50$ μm. With the increase of temperature difference,

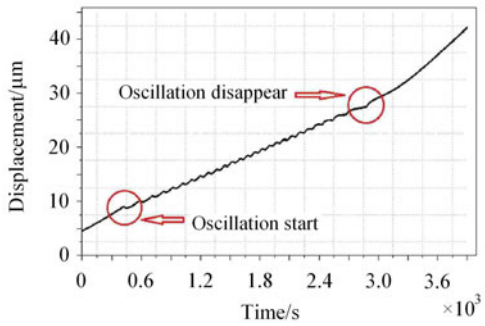

Fig. 3 Typical time (temperature difference)-dependent displacement at test point

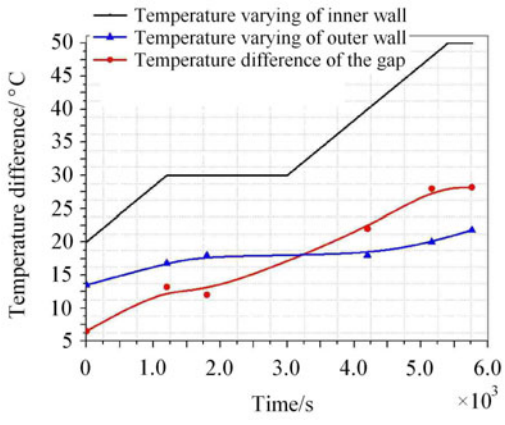

Fig. 4 Temperature difference imposed on the fluid layer (h = 4.5 mm)

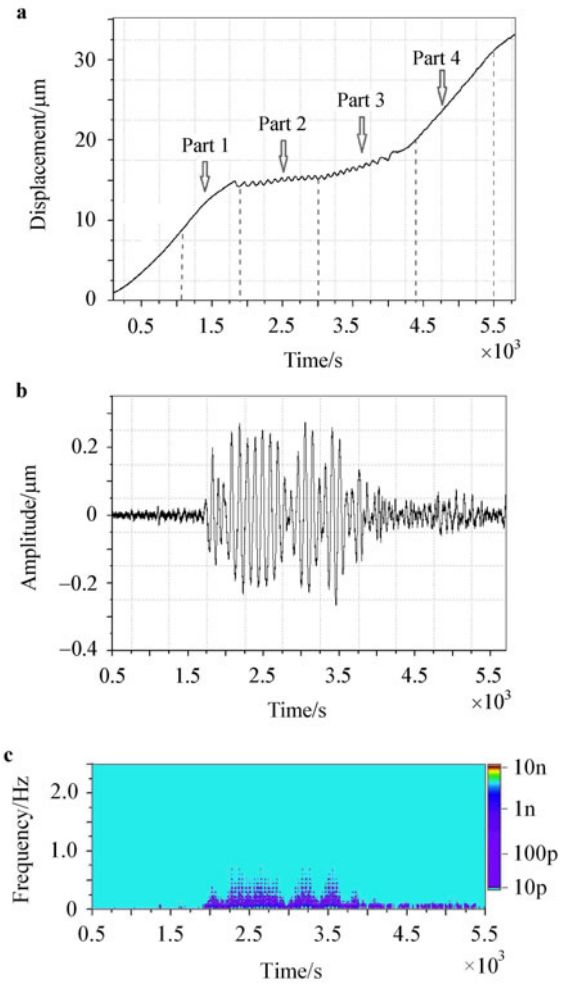

Fig. 5 **a** Time (temperature difference)-dependent displacement (h = 4.5 mm); **b** Oscillation diagram of Fig. 5a; **c** Power spectrum diagram of Fig. 5a

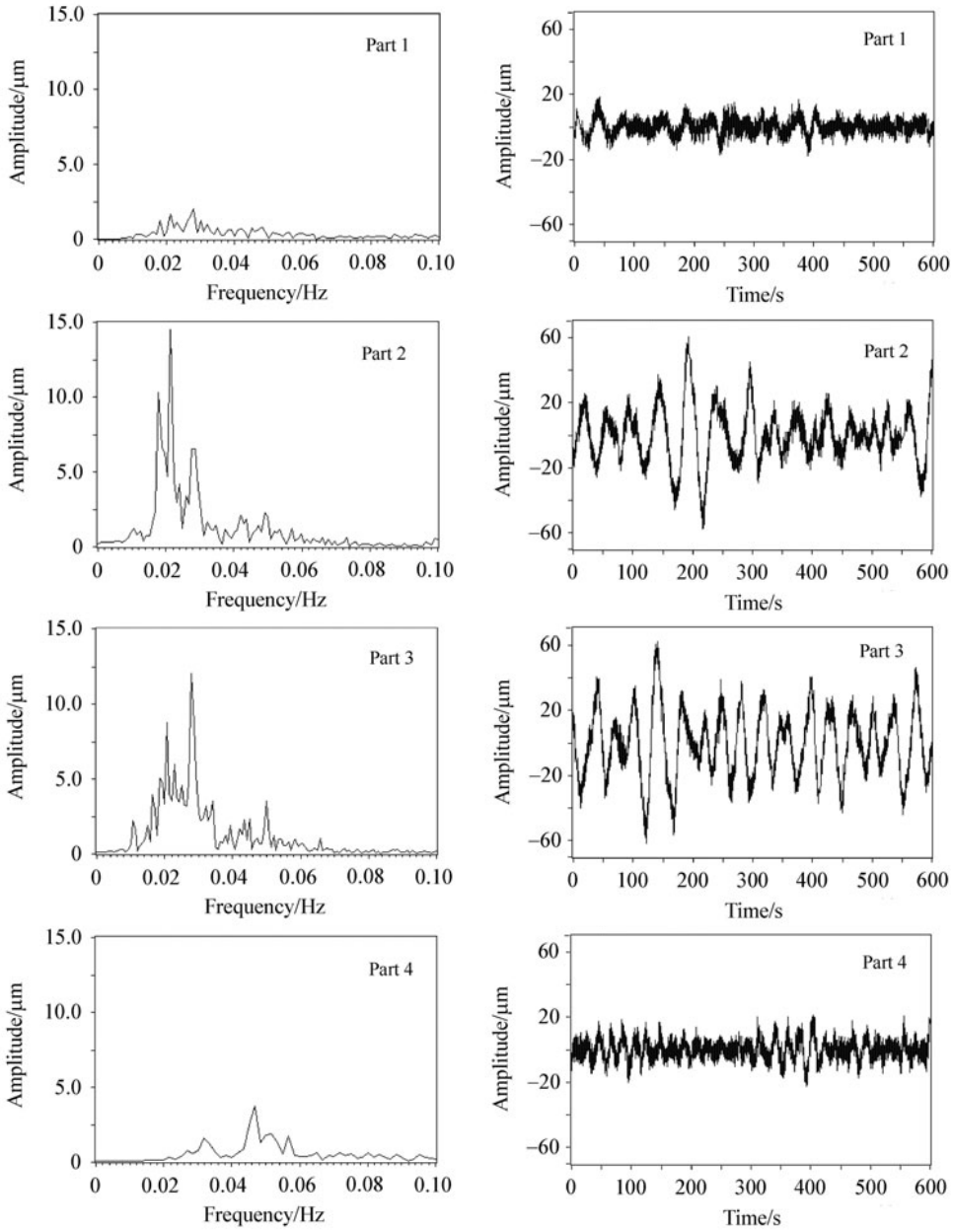

Fig. 6 FFT diagram and oscillation diagram of the divided parts

the dominant frequency changes from 0.021 to 0.028 Hz and the sub-dominant frequency changes from 0.018 to 0.021 Hz. The oscillation seems fiercer than that in Part 2 as the amplitudes grow up.

When it comes to Part 4, the visible oscillation disappears but new higher frequencies show up: $f_5 = 0.032$ Hz, $A_5 = 1.13$ μm, $f_4 = 0.047$ Hz, $A_4 = 2.61$ μm, $f_6 = 0.055$ Hz, $A_6 = 2.00$ μm. They are also very weak but the flow may already come to a new stage of convection because these frequencies are no more the same as those seen in Part 1–Part 3. The visible oscillation disappears when temperature difference is about 23.7°C.

According to the theory of nonlinear dynamics, nonlinear systems have many routes transiting from steady state to unstable state and finally to chaos. One is the so-called "paroxysmal way", which means regular and irregular motions work alternately. From the buoyant-thermocapillary convection system we have studied and the informations given above, regular and irregular signals of surface oscillation appear from time to time when the fluid layer changes to unstable state, which probably indicates that the system is getting to chaos via paroxysmal oscillation.

It reveals almost the same regularity in the range of $0.125 \leqslant A \leqslant 0.375$. So we may give a brief summary here: with the growth of temperature difference, dominant frequency of the visible oscillation will grow too but within certain frequencies. Besides, we find that surface oscillation shares the same frequencies as the temperature oscillation

at the same testing point as well as the same time. So we think that the surface oscillation is another interesting way for us to reveal some important characters of the buoyant-thermocapillary convection besides temperature oscillations and flow visualization.

4 Critical temperature differences

Peng and Kamotani et al. [22, 23] did a ground based buoyant-thermocapillary convection experiment in 1996 and performed STDCE-2 in space 2000, they found that the critical temperature difference (when flow became unstable) showed a different tendence when the container diameter changed ($Pr = 30$, $Hr = 0.1$, $A = 1$). It was convinced that the critical temperature difference seems to be at the same level when the container diameter was near 1.2 cm. Bigger than 1.2 cm, the critical temperature difference will go down under microgravity but reverse under $1g$. This means that when $h = A\ (R_o – R_i) = 5.4$ mm, the role of buoyancy comes out as an important convective driving force which cannot be ignored. In our experiment, $0.125 \leqslant A \leqslant 0.375$, $Hr = 0.2$, R_o and R_i are fixed. The result shows that with the increase of layer thickness from 2.5–7.5 mm, the critical temperature difference for surface oscillation experiences firstly a climb then a decline, as shown in Fig. 7. The turning point lies between 4.5–5.0 mm. We think it implies that the destabilization influence of buoyancy is relatively prominent when the layer thickness is above 5.0 mm. Actually, the flow motion is much more stable as buoyancy grows stronger when the layer is thinner than 4.5 mm. On the contrary, the flow will easily lose stability when the layer is thicker than 5.0 mm because of the increased buoyancy. Our work may be a supplement to the topic since fluids with super high Pr (909) have not been studied well.

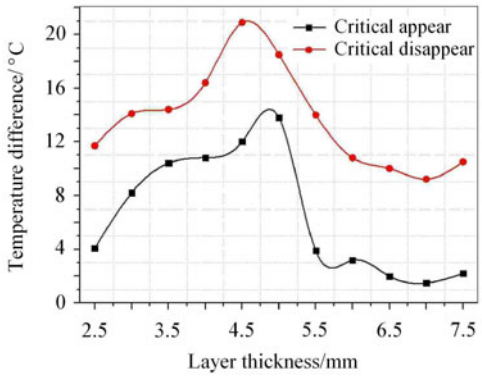

Fig. 7 Critical appearing and disappearing temperature as the layer grows thicker ($Hr = 0.2$, $A = 0.125$–0.375, $Pr = 909$)

Many oscillatory convection related studies have announced the onset of temperature perturbation [22, 23], but none has declared its disappearance after a period of time. As the oscillation characters shown above, main frequencies from FFT analysis are showing an enhancing trend during the whole process of surface oscillation. The visible amplitude does not seem to ease up as the surface oscillation suddenly comes to an end. After its disappearrance, displacement at the signal point is increasing just because of the volume expansion. We think maybe it is an exact critical condition for instability mode to transit from surface wave to hydrodynamic wave or just another stable state, which needs the whole thermo pattern configuration to testify. But to some extent, we have already found that when Bo is small, usually less than 0.3, only thermo oscillations could be explored, which means that convection is represented by hydrodynamic waves not surface waves. Untill a large Bo, almost more than 3, only surface oscillation signals are captured. Here we could get both of them as we claimed sharing the same frequencies using thermocouple observation together within the range of the layer thickness. The reason why oscillations disappear may be understood as the fact that the buoyancy and thermocapillarity can not achieve a certain coupling way to drive the convection regularly. Weak disharmonic signals are found during the irregular motion when the surface oscillations "disappear", but we are not sure whether it would oscillate obviously again once the temperature difference rises even higher beyond the present range ($0\,\text{K} \leqslant \Delta T \leqslant 35.0\,\text{K}$). It is not easy to keep a large temperature difference because of quick heat diffusion in the narrow gap. All these critical problems we discussed here are based on the first time oscillations appearrance and disappearrance.

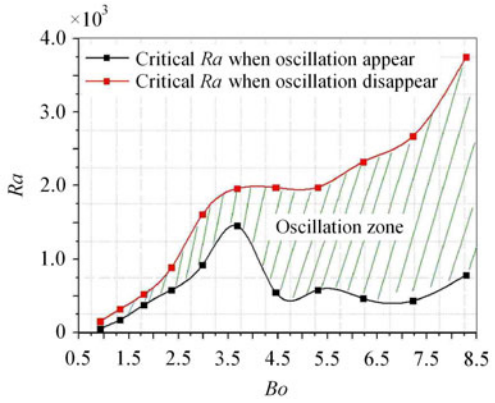

Fig. 8 Relationship between Ra and Bo

Kamotani et al. [24, 25] also suggested that we should not only use Ma to symbolize the appearance of oscillation when the buoyancy was too small and could be ignored, but could use Bo to specify oscillation beginning when buoyancy should not be ignored. In our work, the model is not small enough to reduce the influence of buoyancy and the fluid layer is also not thin enough to ignore buoyancy. So, from the relationship between Ra and Bo as Fig. 8 shows, we can see an interesting phenomenon: the surface oscillation or the unsteady fluid oscillation is restricted within a region which is restricted by the boundaries for appearrance and disappearrance. As pointed out, the region looks quite like a narrow gap when Bo is smaller than 3.7. Meanwhile,

Ra is growing quickly in this period which could be considered as a sign of growing strength of buoyancy. On the other hand, when *Bo* is above 4.5, oscillation state suddenly dumps into a wide area which is quite different from what it is when *Bo* is below 4.5. The fluid easily gets to oscillation as *Ra* surpasses 500, and at the same time the disappearrance boundary shows that the motion is still very sensitive to the change of buoyancy.

5 Conclusions

We carried out an experiment on surface oscillation of buoyant-thermocapillary convection in an open cylindrical annulus. Experimental results can be summarized as follows:

(1) Based on the signal process of surface oscillation for $h = 4.5$ mm, we provide a general description of what kind of procedures and characters the fluid motion will follow as the temperature difference grows. With the growth of temperature difference, dominant frequency of the visible oscillation will grow too but within certain frequencies.

(2) The appearing and disappearing courses during the oscillation show two different transition patterns which are of great significance to study further. It is probably a paroxysmal route for the system to transit to chaos. From Fig. 7, we think that the "balance" point for buoyancy and thermocapillarity exists when the fluid layer thickness is between 4.5 mm–5.0 mm.

(3) As to the relationship between *Ra* and *Bo*, we find that the surface oscillation or unsteady fluid oscillation region is restricted within a narrow gap when *Bo* is smaller than 3.7; but when *Bo* is above 4.5, the fluid easily gets to oscillation as *Ra* surpasses 500.

References

1 Yang, Y.K., Kou, S.: Temperature oscillation in a tin liquid bridge and critical Marangoni number dependency on Prandtl number. Journal of Crystal Growth **222**, 135–143 (2001)

2 Duan, L., Kang, Q., Hu, W.R.: Characters of surface deformation and surface wave in thermal capillary convection. Science in China Series E: Technological Sciences **49**, 601–610 (2006)

3 Hu, W.R., Xu, C.S.: Microgravity Fluid Mechanics. Science Publishing House, Beijing (1999)

4 Benz, S., Schwabe, D.: The three-dimensional stationary instability in dynamic thermocapillary shallow cavities. Experiments in Fluids **31**, 409–416 (2001)

5 Schwabe, D.: Buoyant-thermocapillary and pure thermocapillary convective instabilities in Czochralski systems. J. Crystal Growth **237–239**, 1849–1853 (2002)

6 Schwabe, D., Zebib, A., Sim, B.C.: Oscillatory thermocapillary convection in open cylindrical annuli. I. Experiments under microgravity. J. Fluid Mech. **491**, 239–258 (2003)

7 Schwabe, D., Möller, U., Schneider, J., et al.: Instabilities of shallow dynamic thermocapillary liquid layers. Phys. Fluids A **4**, 1989–1993 (1992)

8 Mizev, A.I., Schwabe, D.: Convective instabilities in liquid layers with free upper surface under the action of an inclined temperature gradient. Physics of Fluids **21**, 112102 (2009)

9 Shi, W.Y., Li, Y.R., Peng, L., et al.: Imaishi: Intrinsical characters of hydrothermal waves in shallow cylindrical annuli. Chinese Journal of Computational Mechanics **26**, 59–65 (2009) (in Chinese)

10 Li, Y.R., Wang, S.C., Shi, W.Y., et al.: Approximate solution to double thin fluid layers thermocapillary convection in cylindrical annuli. Chinese Journal of Theoretical and Applied Mechanics **42**, 306–311 (2010) (in Chinese)

11 Peng, L., Li, Y.R., Zeng, D.L.: Imaishi: Buoyant-thermocapillary convection in cylindrical annuli with medium Pr fluid. Acta Mechanica Sinica **37**, 266–271 (2005) (in Chinese)

12 Peng, L., Li, Y.R., Shi, W.Y., et al.: Three-dimensional thermocapillary-buoyancy flow of silicone oil in a differentially heated annular pool. International Journal of Heat and Mass Transfer **50**, 872–880 (2007)

13 Shi, W.Y., Li, G.Y., Liu, X., et al.: Thermocapillary convection and buoyant-thermocapillary convection in the annular pools of silicon melt and silicone oil. J. Supercond. Nov. Magn. **23**, 1169–1172 (2010)

14 Leppinen, M.D.: Natural convection in a shallow cylindrical annuli. International Journal of Heat and Mass Transfer **45**, 2967–2981 (2002)

15 Kang, Q., Duan, L., Hu, W.R.: Experimental study of surface deformation and flow pattern on buoyant-thermocapillary convection. Microgravity Sci. Technol. **XV/2**, 18–24 (2004)

16 Duan, L., Kang, Q., Sun, Z.W., et al.: The real-time Mach-Zehnder interferometer used in space experiment. Microgravity Sci. Technol. **20**, 91–98 (2008)

17 Duan, L., Kang, Q., Hu, W.R.: Experimental study on liquid free surface in buoyant-thermocapillary convection. Chin. Phys. Lett. **25**, 1347–1350 (2008)

18 Zhu, P., Zhou, B., Duan, L., et al.: Characteristics of surface oscillation in thermocapillary convection. Experimental Thermal and Fluid Science **35**, 1444–1450 (2011)

19 Mo, D.M., Li, Y.R., Shi, W.Y.: Linear-stability analysis of thermocapillary flow in an annular two-layer system with upper rigid wall. Microgravity Sci. Technol. **23**, S43–S48 (2011)

20 Hoyas, S., Herrero, H., Mancho, A.M.: Thermocapillary and thermogravitatory waves in a convection problem. Theoret. Comput. Fluid Dynamics **18**, 309–321 (2004)

21 Bauer, H.F., Eidel, W.: Thermocapillary convection in an annular cylindrical container. Heat Mass Transfer **43**, 217–232 (2007)

22 Kamotani, Y., Masud, J., Pline, A.: Oscillatory convection due to combined buoyancy and thermocapillarity. Journal of Thermophysics and Heat Transfer **10**, 102–108 (1996)

23 Kamotani, Y., Ostrach, S., Masud, J.: Microgravity experiments and analysis of oscillatory thermocapillary flows in cylindrical containers. J. Fluid Mech. **410**, 211–233 (2000)

24 Kamotani, Y., Ostrach, S., Pline, A.: Analysis of velocity data taken in surface tension driven convection experiment in microgravity. Phys. Fluids **6**, 3601–3609 (1994)

25 Kamotani, Y., Ostrach, S., Pline, A.: A thermocapillary convection experiment in microgravity. Journal of Heat Transfer **117**, 611–618 (1995)